THE JOURNAL OF BIOLOGICAL CHEMISTRY VOL. 283, NO. 48, pp. 33267–33275, November 28, 2008


# Following the Path of a Twin-arginine Precursor along the TatABC Translocase of *Escherichia coli*[*]

Received for publication, June 2, 2008, and in revised form, September 25, 2008 Published, JBC Papers in Press, October 3, 2008, DOI 10.1074/jbc.M804225200

**Sascha Panahandeh[‡§], Carlo Maurer[‡], Michael Moser[‡], Matthew P. DeLisa[¶], and Matthias Müller[‡1]**

*From the [‡]Institut für Biochemie und Molekularbiologie, ZBMZ, and the [§]Fakultät für Biologie, Universität Freiburg, D-79104 Freiburg, Germany and the [¶]School of Chemical and Biomolecular Engineering, Cornell University, Ithaca, New York 14853*

**The twin-arginine translocation (Tat) machinery present in bacterial and thylakoidal membranes is able to transport fully folded proteins. Consistent with previous *in vivo* data, we show that the model Tat substrate TorA-PhoA is translocated by the TatABC translocase of *Escherichia coli* inner membrane vesicles, only if the PhoA moiety was allowed to fold by disulfide bond formation. Although even unfolded TorA-PhoA was found to physically associate with the Tat translocase of the vesicles, site-specific cross-linking revealed a perturbed interaction of the signal sequence of unfolded TorA-PhoA with the TatBC receptor site. Some of the folded TorA-PhoA precursor accumulated in a partially protease-protected membrane environment, from where it could be translocated into the lumen of the vesicles upon re-installation of an $H^+$-gradient. Translocation arrest occurred in immediate vicinity to TatA. Consistent with a neighborhood to TatA, TorA-PhoA remained protease-resistant in the presence of detergents that are known to preserve the oligomeric structures of TatA. Moreover, entry of TorA-PhoA to the protease-protected environment strictly required the presence of TatA. Collectively, our results are consistent with some degree of quality control by TatBC and a recruitment of TatA to a folded substrate that has functionally engaged the twin-arginine translocase.**

The twin-arginine translocation (Tat)[2] pathway is a protein transport system of bacteria, archaea, and chloroplasts that possesses the ability to export proteins in a fully folded conformation. Proteins are targeted to the Tat pathway by N-terminal signal peptides that contain an almost invariant twin-arginine sequence motif. Pretranslocational folding results from the cytosolic incorporation of metallo cofactors and assembly into oligomeric complexes or even merely from rapid folding kinetics. Tight folding, however, is not a prerequisite for export via the Tat pathway (1–3). Many Tat systems comprise three functionally distinct membrane proteins, the single-span TatA and TatB, and the polytopic TatC. In contrast, Gram-positive bacteria possess only TatA and TatC with TatA functionally replacing TatB. Consistent with this peculiarity of Gram-positive TatAs, distinct N-terminal amino acid substitutions of *Escherichia coli* TatA render it bifunctional and suppress a TatB deficiency (4, 5).

TatB and TatC form 360–700-kDa complexes (6, 7) without participation of TatA (8, 9). Heterodimeric TatBC complexes represent functional units (10) and assemble into oligomeric structures that center around a TatB core (11, 12). Within the TatBC complex, TatC functions as primary recognition site for RR signal sequences (13–15). Precursor recognition involves epitopes within the entire N terminus of TatC (16–18).

TatA mediates the actual translocation event. It is the most abundant Tat component that assembles into homo-oligomeric complexes varying in size from less than 100 kDa up to 700 kDa (19–22). Single particle electron microscopy of purified *E. coli* TatA complexes revealed pore-like structures with a lid-like element presumably formed by the amphipathic helices of TatA (23). Circumstantial evidence for transient rearrangements of this amphipathic helix has been provided (22, 24, 25), and the currently available data support the concept of a size-fitting TatA pore, which would be formed by, or recruited to, the precursor-TatBC complex in a $\Delta\mu_H{}^+$ (proton-motive force)[5]-dependent manner (22, 26). In contrast, recent findings of a membrane-spanning Tat intermediate, which was not found in close proximity to any Tat component (3), and of abolished transport for a Tat substrate protein exposing hydrophobic side chains on its surface (2) would support transmembrane passages occuring next to membrane lipids, with TatA possibly functioning by destabilizing the rigid lipid bilayer (27).

Besides diverging views on the actual translocation event, quality control is another point of contention. To date, experimental evidence has been provided for both discrimination against, and tolerance toward, unfolded substrates by Tat translocases. The disulfide-harboring alkaline phosphatase (PhoA) when equipped with a Tat signal peptide is exported in a Tat-dependent manner exclusively from *E. coli* mutant strains that enable oxidative protein folding in the cytoplasm (28). Likewise, Tat-mediated transport of cytochrome *c* into the periplasm was found to occur only when maturation and folding in the cytoplasm was possible (29).

* This work was supported by Grant LSHG-CT-2004-005257 of the European Union (to S. P. and M. M.), grants from the Deutsche Forschungsgemeinschaft (Collaborative Research Centres 388 and 746, to M. M.), an F.F. Nord fellowship of the University of Freiburg (to C. M.), and an NSF Career Award (CBET 0449080) and a NYSTAR James D. Watson Award (both to M. P. D.). The costs of publication of this article were defrayed in part by the payment of page charges. This article must therefore be hereby marked "*advertisement*" in accordance with 18 U.S.C. Section 1734 solely to indicate this fact.

[1] To whom correspondence should be addressed. Tel.: 49-761-203-5265; Fax: 49-761-203-5274; E-mail: matthias.mueller@biochemie.uni-freiburg.de.

[2] The abbreviations used are: Tat, twin-arginine translocation; AMS, 4-acetamido-4′-maleimidylstilbene-2,2′-disulfonic acid; *p*Bpa, *p*-benzoyl-L-phenylalanine; $C_{12}E_9$, nona-polyoxyethylene dodecyl ether; CCCP, carbonyl cyanide *m*-chlorophenyl-hydrazone; Chaps, 3-[(3-cholamidopropyl)dimethyl-ammonio]-1-propanesulfonate; DCCD, *N*,*N*′-dicyclohexylcarbodiimide; DFP, diisopropyl fluorophosphate; $\Delta\mu_H{}^+$, proton-motive force; IAA, iodoacetamide; INVs, inverted vesicles; OG, octylglucoside; PhoA, alkaline phosphatase; PK, proteinase K; DTT, dithiothreitol.

These results would be consistent with a quality-of-folding control directly carried out by the Tat translocon. This concept was, however, challenged by the finding that even reduced and unfolded PhoA associates with the TatBC complex via a Tat signal sequence (30). *E. coli* cells overexpressing such transport-incompatible substrate display a defective proton gradient, which the authors attributed to a faulty translocation of unfolded PhoA, seemingly excluding the existence of a quality control by TatABC (30). A proofreading system involving the TatABC apparatus, which seems to be unique for defectively folded RR-dependent Fe/S proteins of *E. coli*, was recently described (31).

Here we have reproduced *in vitro* the Tat-dependent transport of PhoA fused to the RR-signal sequence of TMAO (trimethylamine *N*-oxide) reductase (TorA). We find that much like *in vivo*, unfolded precursor specifically associates with the Tat translocase, but is not further translocated into cytoplasmic membrane vesicles of *E. coli*. Binding to TatBC differs however, between folded and unfolded precursors suggesting a discriminatory ability of TatBC. These studies also allowed some insights into the path of a Tat precursor following its recognition by TatBC up to a step where it is brought in close vicinity to TatA.

## EXPERIMENTAL PROCEDURES

*Plasmids and E. coli Strains*—For the synthesis of pSufI and TorA-PhoA, plasmids pKSMSufI-RR (13) and pET28aTorA-PhoA were used, respectively. For the construction of pET28a-TorA-PhoA, the chimeric gene encoding the TorA signal peptide fused to PhoA was PCR-amplified from plasmid pSALect-ssTorA-PhoA-Bla (32). The resulting PCR product was digested with NcoI and SalI and ligated into the same sites in pET28a (Novagen). The final vector was confirmed to be correct by sequencing. Strain M15pRep4 (Quiagen) transformed with pQE60-TorD (33) was used for the expression of TorD. Plasmid pDULE-*p*Bpa (34) was transformed into strain Top10 (Invitrogen).

*Plasmid Construction*—PCR-based site-specific mutations were introduced using the QuikChange Site-directed Mutagenesis kit system (Stratagene) following the manufacturer's instruction. Plasmid pET28aTorA-PhoA was used as template for the introduction of TAG stop codons at different amino acid positions. For position 15 (Phe) the two complementary oligonucleotides TorA-PhoAF15for (5′-CA TCA CGT CGG CGT TAG CTG GCA CAA CTC GGC GGC-3′) and TorA-PhoAF15rev (5′-GCC GCC GAG TTG TGC CAG CTA ACG CCG ACG TGA TG-3′) were used to give the plasmid pET28aTorA-PhoAF15. Analogously, plasmid pET28aTorA-PhoAV24 was constructed using the complementary oligonucleotides TorA-PhoAV24for (5′-CAA CTC GGC GGC TTA ACC TAG GCC GGG ATG CTG G-3′) and TorA-PhoAV24rev (5′-C CAG CAT CCC GGC CTA GGT TTA GCC GCC GAG TTG-3′).

For synthesis of mutant TorA-PhoA proteins having the arginine 12 and 13 replaced by lysines (TorA-PhoA-KK) stepwise site-specific mutations were performed as described above. In a first reaction the two complementary oligonucleotides TorA-PhoAR12KRfor (5′-CTC TTT CAG GCA TCA AAG CGG CGT TTT CTG GCA CAA CTC GGC-3′) and TorA-PhoAR12KRrev (5′-GCC GAG TTG TGC CAG AAA ACG CCG CTT TGA TGC CTG AAA GAG-3′) and plasmid pET28aTorA-PhoA as template were used to give the plasmid pET28aTorA-PhoAKR. Using this plasmid as template and the two complementary oligonucleotides TorA-PhoAKR13Kfor (5′-CTC TTT CAG GCA TCA AAG AAG CGT TTT CTG GCA CAA CTC GGC-3′) and TorA-PhoAKR13Krev (5′-GCC GAG TTG TGC CAG AAA ACG CTT CTT TGA TGC CTG AAA GAG-3′), plasmid pET28aTorA-PhoAKK was subsequently constructed.

Similarly, the alanines 40 and 41 of TorA-PhoA were stepwise replaced by leucines using plasmid pET28aTorA-PhoA as template and the two complementary oligonucleotides TorA-PhoA40LAfor (5′-CCG CGA CGT GCG ACT CTG GCG CAA GCG GCG-3′) and TorA-PhoA40LArev (5′-CGC CGC TTG CGC CAG AGT CGC ACG TCG CGG-3′) to give pET28aTorA-PhoALA. This plasmid served as template in a second reaction with the two complementary oligonucleotides TorA-PhoLA41Lfor (5′-CCG CGA CGT GCG ACT CTG CTG CAA GCG GCG-3′) and TorA-PhoLA41Lrev (5′-CGC CGC TTG CAG CAG AGT CGC ACG TCG CGG-3′) to give the plasmid pET28aTorA-PhoAΔSP.

*In Vitro Transcription/Translation*—An S-135 was prepared from the *E. coli* strain Top10 (Invitrogen) transformed with plasmid pDULE-*p*Bpa. Cells were grown overnight in the presence of 25 μg/ml tetracycline and used to inoculate at a 1:50 ratio fresh medium supplemented with 2.5 μg/ml tetracycline. Cells were grown and an S-135 prepared according to Ref. 35.

Coupled transcription/translation of SufI and TorA-PhoA from plasmid DNA was performed as described (13) with some modifications. Oxidizing conditions were established by the addition of 5 mM GSSG at the start of the synthesis. Synthesis of stop codon mutants of TorA-PhoA was enabled by adding 40 μM *p*Bpa from a 2 mM aqueous solution that had been diluted from a 1 M stock solution made in 1 M NaOH. For cross-linking experiments, membrane vesicles were added as described (13). To assay transport of SufI and TorA-PhoA, membrane vesicles were added 10 min after starting the synthesis reaction and incubated for 25 min. To assay binding of TorA-PhoA, synthesis was stopped after 30 min, and membrane vesicles were added and incubated for 15 min.

*Preparation of Membrane Vesicles*—INV were prepared according to Ref. 35 from the *E. coli* wild-type strains BL21(DE3)pLysS (36) and MC4100 (37) as well as from the *tat* deletion strain DADE (MC4100, Δ*tatABCD*Δ*tatE*) (38). $Tat^+$-INV were prepared from *E. coli* strain BL21(DE3)pLysS transformed with plasmid p8737 (39) whereas ΔTatA-INV were prepared from *E. coli* strain MC4100 transformed with plasmid pFAT222 (40). *Tat* genes encoded by both plasmids were induced by 2 mM isopropyl thio-β-D-galactopyranoside.

*Cross-linking and Immunoprecipitation*—Cross-linking of *p*Bpa was induced by irradiating samples with UV light of 365-nm wave length for 20 min on ice. Subsequent treatments of samples were performed as described (13). For native immunoprecipitation denaturation by 1% SDS was omitted.

*Thiol Trapping of in Vitro Synthesized TorA-PhoA*—TorA-PhoA was synthesized in a coupled transcription/translation reaction in the presence or absence of 5 mM GSSG. Synthesis was stopped by the addition of trichloroacetic acid to a final concentration of 5% and incubated on ice for 30 min. For alkylation of free sulfhydryl groups the trichloroacetic acid pellet, obtained by centrifugation at 16,000 × *g* for 10 min at room temperature, was washed with 100% acetone. For SDS-PAGE analysis, the washed pellet was dissolved in DTT-free sample buffer supplemented with 100 mM IAA for 30 min at 25 °C. Trichloroacetic acid precipitates obtained by centrifugation for 30 min at 16,000 × *g* at 4 °C were treated with AMS (Molecular Probes) as described (41) and analyzed by reducing SDS-PAGE.

## RESULTS

*In Vitro Reconstruction of the Folding-dependent Export of TorA-PhoA by the Tat Machinery*—We have analyzed *in vitro* the twin-arginine-dependent translocation of the fusion protein TorA-PhoA into inside-out inner membrane vesicles (INV) of *E. coli*. In TorA-PhoA (Fig. 1*A*) the RR motif-bearing signal sequence and the first seven amino acids of the mature part of TorA are fused to mature PhoA. The same construct was previously shown *in vivo* to be exported by the Tat pathway across the inner membrane of *E. coli*, provided that oxidizing conditions were implemented in the cytoplasm to allow prior folding of the PhoA moiety by disulfide bond formation (28).

The precursor of TorA-PhoA and, for comparison, that of a standard Tat substrate, SufI, were *in vitro* synthesized and radioactively labeled by a coupled transcription/translation system prepared from *E. coli*, separated by SDS-PAGE and visualized by phosphorimaging (Fig. 1*B*, *lanes 5* and *1*, respectively). Translocation of SufI into INV is indicated by the accumulation of two discrete proteinase K (PK)-resistant species (compare *lanes 2* and *4*) that correspond in size to the precursor (*p*) and the signal sequence-less, mature form (*m*) of SufI. Consistent with having been processed by signal peptidase, the latter appeared only upon addition of INV (compare *lanes 1* and *3*). As shown previously Tat-dependent translocation of twin-arginine substrates into INV requires overproduced amounts of TatA, -B, and -C in the vesicles ($Tat^+$-INV).

In contrast, no protease-protected TorA-PhoA could be obtained by the same membrane vesicles (*lanes 5* and *6*), unless synthesis of TorA-PhoA was performed under oxidizing conditions. Dependent on increasing amounts of oxidized glutathione (GSSG), three species of TorA-PhoA became increasingly protease-protected (*lanes 8*, *10*, *12*). These correspond in size to the precursor (*p*), the signal sequence-less form (*m*), and a smaller unexpected form (labeled *i*). The identities of the m- and i-forms are revealed below. To demonstrate that translocation of TorA-PhoA into $Tat^+$-INV indeed required folding of the PhoA moiety, thiol-specific labeling of TorA-PhoA was performed (Fig. 1*C*). Alkylation by IAA preserves the reduced state of the PhoA-moiety causing a decreased electrophoretic mobility compared with the more tightly packed oxidized PhoA. Alkylation of TorA-PhoA by IAA was possible only when synthesis had occurred under reducing conditions (*lane 3*). TorA-PhoA synthesized in the presence of 5 mM GSSG, however, could not be modified indicating a lack of free thiols due to disulfide bridge formation. Likewise, an increase in size due to alkylation with the 490 Da compound AMS was only observed if TorA-PhoA retained its SH-groups by synthesis under reducing conditions (*lanes 6* and *8*).

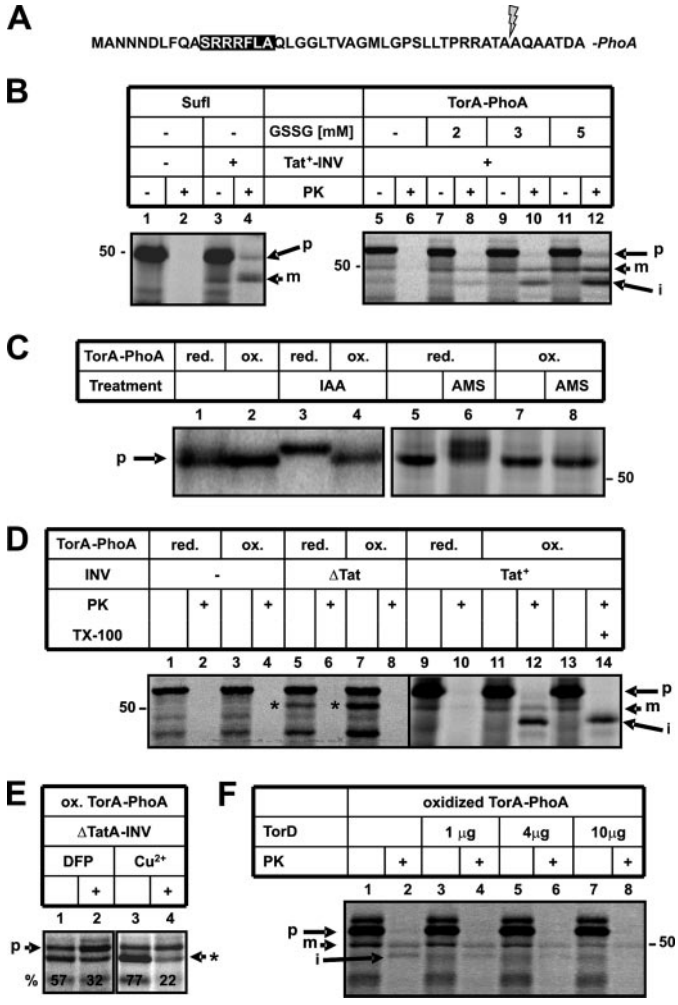


FIGURE 1. **Only when synthesized under oxidizing conditions is TorA-PhoA translocated into *E. coli* membrane vesicles via the TatABC translocase.** *A*, N-terminal amino acid sequence of TorA-PhoA with the RR consensus motif of the signal sequence highlighted by a *black box* and the predicted cleavage site marked by an *arrow*. Note that the cloning procedure introduced an additional Ala residue at position 2 of the authentic TorA signal sequence. *B*, SufI and TorA-PhoA were synthesized *in vitro*, $^{35}S$-labeled translation products were separated by SDS-PAGE and visualized by phosphorimaging. Synthesis was performed either in the presence of DTT (2 mM) or DTT plus the indicated concentrations of oxidized glutathione (*GSSG*). Inside-out inner membrane vesicles prepared from an *E. coli* strain that overproduced TatABC (*$Tat^+$-INV*) were added during synthesis as indicated. Following incubation, 15 μl of each reaction were treated with 5% trichloroacetic acid, whereas 30 μl were first digested with 0.5 mg/ml PK for 25 min at 25 °C. *p* and *m*, denote precursor and mature, *i.e.* signal sequence-less, forms of SufI and TorA-PhoA. *i*, is an intermediate form of TorA-PhoA as detailed in the text. *C*, TorA-PhoA was synthesized under reducing (2 mM DTT) or oxidizing (2 mM DTT and 5 mM GSSG) conditions and thiol trapping was performed with the alkylating reagents *IAA* and *AMS* as detailed under "Experimental Procedures." *D*, TorA-PhoA was synthesized under the indicated conditions. Triton X-100 was added to a final concentration of 1% during PK treatment. ΔTat-INV were obtained from an *E. coli* strain lacking TatA, -B, -C, -D, and -E. These vesicles caused some translocation-independent pseudo-processing of TorA-PhoA (*). *E*, pseudo-processing decreases in the presence of the OmpT inhibitors DFP (50 mM) and copper ions (5 mM $CuCl_2$). *F*, His-tagged TorD was purified and added at the indicated amounts during synthesis of TorA-PhoA.

Much like the situation *in vivo*, oxidized TorA-PhoA was only translocated across the cytoplasmic membrane into the

lumen of INV, and thereby acquired protease-resistance, if the vesicles contained an active Tat machinery (Fig. 1*D*). No PK-resistant material was obtained in the presence of INV prepared from a *tatABCDE* deletion mutant (ΔTat-INV) (compare *lanes 8* and *12*). These vesicles, however, produced a cleaved form of TorA-PhoA (marked with an *asterisk*). This form was suspicious of being the cleavage product of OmpT rather than that of signal peptidase, because the signal sequence of TorA contains a potential cleavage site of OmpT between two distal arginine residues (cf. Fig. 1*A*) and different from $Tat^+$-INV, the ΔTat-INV had not been prepared from an *ompT* deletion strain. In fact, the ratio of pseudo-processed TorA-PhoA to precursor was decreased by the OmpT inhibitors DFP und $Cu^{2+}$ ions (Fig. 1*E*).

Collectively, the results shown in Fig. 1 indicate that similar to the situation *in vivo*, the Tat apparatus of INV is able to translocate TorA-PhoA only when the PhoA moiety is folded due to disulfide bond formation. The authenticity of this transport event is underscored by the finding that it was competitively inhibited by the TorA-specific chaperone TorD (Fig. 1*F*), the anti-targeting activity of which has been described (42).

*The TatABC Translocase Senses the Folding State of TorA-PhoA*—One obvious question arising from the above findings is, by which mechanism is translocation of reduced TorA-PhoA prevented. We first examined physical association of TorA-PhoA with the TatABC translocase of INV. As shown in Fig. 2*A*, TorA-PhoA synthesized under oxidizing conditions and in the absence of INV eluted from Sepharose CL-6B as a broad peak (*fractions 10–15*, ▲). Translocation of TorA-PhoA into $Tat^+$-INV (cf. *control lanes*) coincided with the appearance of a second peak of TorA-PhoA eluting earlier (fractions 6–8, ▲). This peak was absent from a sample containing ΔTat-vesicles (□) and therefore must represent TorA-PhoA both targeted to and translocated by the TatABC translocase. The translocated material could be visualized when all fractions were treated with proteinase K (not shown).

An identical TatABC-dependent membrane-association was also obtained for the reduced form of TorA-PhoA (Fig. 2*B, fractions 6–8,* ▲), consistent with a previous report (30). Not even replacement of the essential twin-arginine pair by two consecutive lysines prevented the reduced form of TorA-PhoA from binding to $Tat^+$-INV (Fig. 2*C*). Thus membrane association of TorA-PhoA mediated by TatABC seemed to be affected neither by a translocation-incompetent PhoA moiety nor by an inactive TorA signal sequence.

We previously demonstrated by site-specific cross-linking that targeting of SufI to TatBC of *E. coli* was disturbed if the signal sequence was rendered transport-incompetent by introducing a KK mutation. We therefore wondered whether targeting of TorA-PhoA that was rendered transport-incompetent due to reductive unfolding would result in identical cross-links to TatC and TatB, *i.e.* molecular contacts, as the transport-active oxidized TorA-PhoA. To investigate this in detail, we replaced the codons for Phe-15 and Val-24 of the TorA-PhoA signal sequence (cf. Fig. 3*A*) by amber stop codons in the TorA-PhoA-encoding plasmid. To suppress these stop codons, *in vitro* synthesis of the mutant forms of TorA-PhoA was performed by a cell-free extract that had been prepared from an *E. coli* strain transformed with plasmid pDULE (34). This plasmid encodes the orthogonal pair of an amber suppressor tRNA, which specifically accepts the photoreactive derivative of Phe, *p*-benzoyl-L-phenylalanine (*p*Bpa), as well as its cognate *p*Bpa-specific aminoacyl-tRNA synthetase (43). Under these conditions only by addition of *p*Bpa can the stop codons present in the mutant *torA-phoA* mRNAs be suppressed, giving then rise to full-size translation products with the photoprobe *p*Bpa incorporated at the respective positions (Fig. 3*B*, *pF15-TorA-PhoA* and *pV24-TorA-PhoA*).

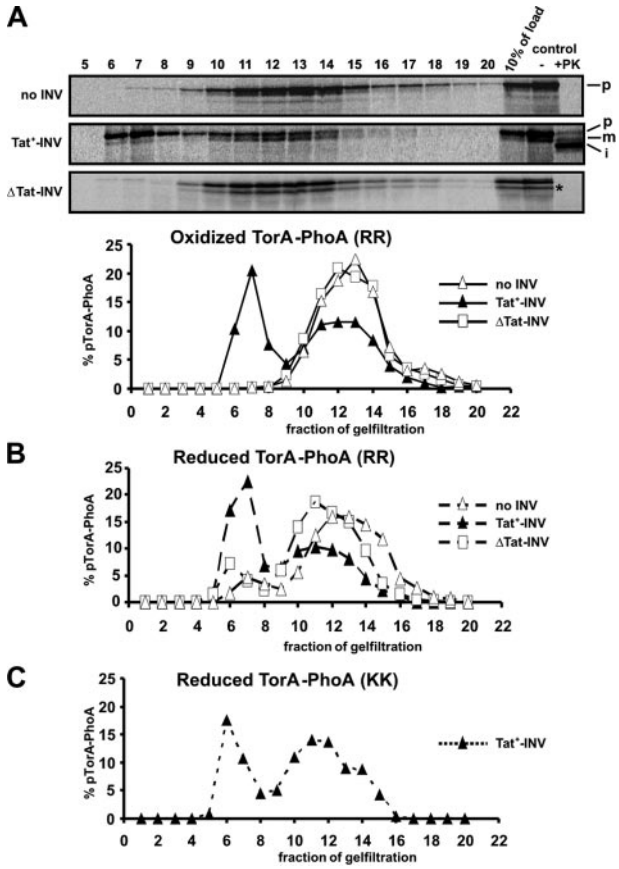


FIGURE 2. **TatABC-dependent membrane association of translocation-competent and translocation-incompetent forms of TorA-PhoA.** *A*, TorA-PhoA was synthesized *in vitro* under oxidizing conditions in the absence or presence of *INV* and reactions were stopped by 0.8 mM puromycin. Translocation was assessed as depicted in the *control* lanes. After removing aggregated material by centrifugation at 16,000 × *g* for 20 min at 4 °C, 100-μl reaction volumes were applied to a 1.5 ml Sepharose CL-6B column and eluted in 20 × 100 μl fractions, which together with 10% of the load were analyzed by SDS-PAGE. INV uniquely eluted in fractions 6–8 as confirmed by the presence of PK-resistant material (not shown). The radioactivity of each fraction was quantitated using Image Quant 5.2 software (Molecular Dynamics) and the means of 2–5 parallel experiments were plotted. The diagram illustrates the peak of membrane-associated TorA-PhoA only in those assays that contained $Tat^+$-INV. *B,* same as in *A* for TorA-PhoA now synthesized under reducing conditions. Despite the fact that reduced TorA-PhoA is not competent for translocation it associated with $Tat^+$-INV in much the same manner as the oxidized TorA-PhoA depicted in *panel A*. *C*, membrane association of the KK mutant of TorA-PhoA synthesized under reducing conditions. These data were obtained from a single experiment. Even inactivation of the signal sequence by replacing the RR-consensus with a KK pair does not prevent TorA-PhoA from binding to $Tat^+$-INV.

The *p*Bpa-containing TorA-PhoA species were synthesized both under reducing and oxidizing conditions and subsequently irradiated with UV light. In the absence of membrane

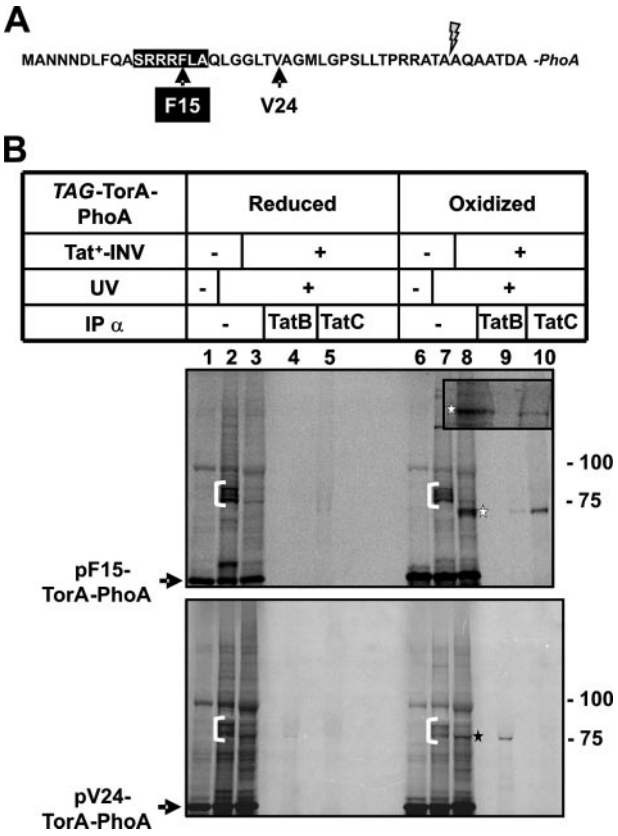


FIGURE 3. **Impaired recognition of reduced TorA-PhoA by TatB and TatC.** *A*, amino acids within the signal sequence of TorA-PhoA that were replaced by *p*Bpa, a UV-sensitive derivative of phenylalanine. *B*, TorA-PhoA DNA, in which the codons either for Phe-15 or Val-24 had been replaced by TAG stop codons, was expressed *in vitro* in the presence of a UAG-suppressor tRNA, the cognate *p*Bpa-specific aminoacyl-tRNA synthetase, and *p*Bpa. Synthesis of the TorA-PhoA mutants was performed both under reducing and oxidizing conditions, as indicated. Cross-linking was induced by UV-irradiation and adducts were immunoprecipitated using antibodies directed against TatB and TatC. The cross-link to TatC is labeled with an *open star*, that to TatB with a *black star*. *White brackets*, adducts of TorA-PhoA obtained in the absence of INV. The *inset* shows a magnification of the *open star*-labeled band in lanes 8–10 from an independent experiment.

vesicles, a number of adducts were obtained (Fig. 3*B*, *lanes 2* and *7*, *brackets*). These cross-linking products faintly cross-reacted with antibodies against the chaperones FkpA and TorD (not shown) reflecting the free accessibility of the TorA signal sequence to chaperone-like proteins when it was not bound to TatABC. In the presence of $Tat^+$-INV, however, oxidized TorA-PhoA yielded a 70-kDa adduct for the cross-linker positioned at residue Phe-15 (Fig. 3*B*, *lane 8*, *open star*), and a 75-kDa adduct (*black star*) when *p*Bpa was incorporated at position Val-24 of the TorA signal sequence. The two cross-linking partners were identified by immunoprecipitation as TatC (*lane 10*) and TatB (*lane 9*; the weak signal in *lane 9*, *upper panel* is not due to cross-reactivity between the two antisera used, as demonstrated by an independent experiment shown in the *inset*). Thus the TorA signal sequence of oxidized TorA-PhoA displayed the same contacts to TatB and TatC as previously described for preSufI (13). In marked contrast, the reduced form of TorA-PhoA yielded only faint TatB- and TatC-specific adducts (Fig. 3*B*, *lanes 3–5*) indicating that, although translocation-incompetent TorA-PhoA physically associates with TatABC of *E. coli*, its molecular contacts to TatB and TatC differ from those of the translocation-competent counterpart. Therefore, TatBC as the receptor site of the Tat translocase seems to be able to sense the folding state of PhoA.

*In Vitro Translocation of Oxidized TorA-PhoA Yields a Translocation-arrested Fragment*—As shown above (see Fig. 1*B*, *lane 12*), a substantial fraction of oxidized TorA-PhoA, which became protease-protected in the presence of Tat-competent membrane vesicles, displayed a faster electrophoretic mobility than the signal sequence-less m-form. The appearance of this i-species strictly depended on translocation-proficient conditions, *i.e.* a folded substrate and TatABC-containing vesicles (see Fig. 1*D*, *lanes 8*, *10*, and *12*). Thus, the circumstances of its occurrence together with its reduced size suggest that it reflected a partially translocated form of TorA-PhoA. We next characterized this translocation-arrested fragment (i-species) of TorA-PhoA in more detail.

In contrast to precursor and mature TorA-PhoA, this smaller species did not disappear when PK treatment was performed in the presence of 1% Triton X-100 to disrupt the integrity of the vesicles (Fig. 1*D*, *lanes 12* and *14*) indicating that it was not accessible from the periplasmic side of the membrane.

When the translocation kinetics of oxidized TorA-PhoA into $Tat^+$-INV were recorded (Fig. 4*A*), it became evident that the accumulation of the translocation-arrested fragment was retarded with respect to that of the fully translocated precursor and mature form of TorA-PhoA. This behavior would be expected if translocation arrest was due to a gradual overload of the INVs' TatABC translocase with the substrate TorA-PhoA.

Fig. 4*B* demonstrates that a proteolytic fragment with the same electrophoretic mobility was obtained from a TorA-PhoA precursor, whose signal peptide cleavage site had been removed by mutation. As expected no processed mature form (*m*) appeared after PK treatment of ΔSP-TorA-PhoA (compare *lanes 4* and *6*), which incidentally identifies the m-species of wild-type TorA-PhoA as the signal sequence-less form (see above). Despite the absence of the m-band from the PK-lane of ΔSP-TorA-PhoA, the i-form was generated by PK from the non-cleavable mutant (*lane 6*). This result together with the pronounced intensity of the i-form suggests that it was derived from the precursor TorA-PhoA, and that translocation arrest occurred prior to cleavage of the signal sequence.

To find out where in the TorA-PhoA sequence PK cleaved to yield the translocation-arrested fragment, we made use of the C-terminal His tag of TorA-PhoA. As depicted in Fig. 4*C*, both the precursor and the mature form of TorA-PhoA were immunoprecipitated by anti-His tag antibodies (*lanes 1* and *3*), but not the i-form (*lanes 2* and *4*). Hence this species must have lost its His tag during digestion with PK because of an unprotected C terminus of the translocation-arrested fragment of TorA-PhoA.

Importantly, the appearance of the partially translocated form of TorA-PhoA was strictly dependent on a correct membrane targeting. This is indicated by its loss upon inactivation of the signal sequence (Fig. 5*A*). Changing the consensus RR-motif in the signal sequence of TorA-PhoA to a KR pair decreased the amount of translocation-arrested fragment obtained (compare *lanes 2* and *4*) and replacement by a KK pair completely abolished its appearance (*lane 6*). Translocation arrest must

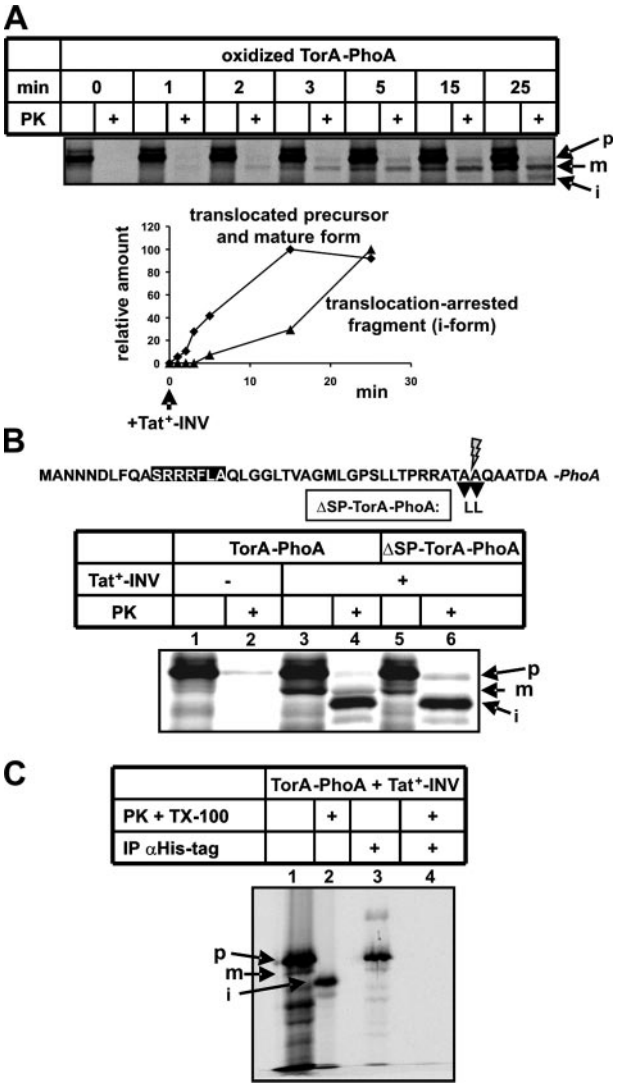


FIGURE 4. **The translocation-arrested fragment of TorA-PhoA, presumably resulting from an overload of the TatABC translocase, contains the signal sequence but has an unprotected C terminus.** *A*, time course of translocation into *Tat*$^+$*-INV* of TorA-PhoA synthesized *in vitro* under oxidizing conditions. *B*, *in vitro* synthesis of TorA-PhoA and the non-cleavable mutant ΔSP-TorA-PhoA under oxidizing conditions and translocation into Tat$^+$-INV. *C*, His-tagged TorA-PhoA synthesized under oxidizing conditions and in the presence of Tat$^+$-INV (*lane 1*) was denaturated with 1% SDS at 56 °C for 10 min and subsequently applied to anti-His antibody-loaded protein A-Sepharose (*lane 3*). To generate the iTorA-PhoA fragment a parallel sample was treated with PK and 1% Triton X 100 (*lane 2*) and following inactivation of PK, denaturated with 1% SDS and applied to anti-His antibody-loaded protein A-Sepharose (*lane 4*).

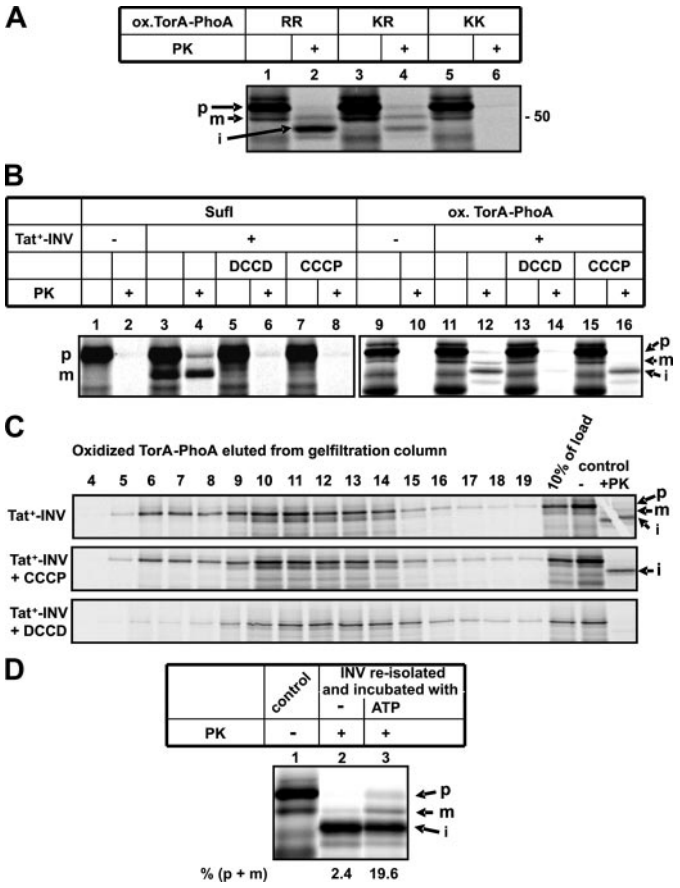


FIGURE 5. **Translocation arrest of TorA-PhoA requires a functional targeting to the Tat translocase.** *A*, oxidized TorA-PhoA containing the wild-type RR motif as well as its KR and KK variants were analyzed for complete and partial translocation into Tat$^+$-INV. *B*, effect of DCCD (0.5 mM) and CCCP (0.1 mM) on complete and partial translocation of SufI and oxidized TorA-PhoA into Tat$^+$-INV. Stock solutions of both drugs were prepared in DMSO, which was added in equivalent amounts to control reactions. *C*, in contrast to CCCP, DCCD interferes with binding of oxidized TorA-PhoA to Tat$^+$-INV. For experimental details see Fig. 2. *D*, oxidized TorA-PhoA was synthesized in the presence of Tat$^+$-INV (*control*). INV were reisolated by centrifugation at 100,000 × *g* for 30 min at 4 °C and resuspended in compensating buffer (35) containing 3.2% (w/v) polyethylene glycol 6000, 2 mM DTT, 5 mM GSSG, and either no further additives or an ATP-regenerating system, and incubated for 25 min at 37 °C before PK treatment.

therefore occur at a step beyond functional targeting to the TatBC receptor site of the translocase. It did, however, occur prior to the $\Delta\mu_H^+$-dependent event(s) of Tat-specific translocation. This was elucidated by the use of two inhibitors of the $\Delta\mu_H^+$, *CCCP* and *DCCD* (Fig. 5*B*). CCCP dissipates $\Delta\mu_H^+$ by acting as protonophore, while DCCD interferes with the ATP-dependent generation of $\Delta\mu_H^+$ by the vesicles via a covalent modification of the c subunit of the $F_1F_O$-ATPase. Both inhibitors block the formation of translocated, *i.e.* PK-resistant, precursor and m-form of the control Tat substrate SufI (Fig. 5*B*, *lanes 4*, *6*, and *8*) and of oxidized TorA-PhoA (*lanes 12*, *14*, and *16*). Accumulation of the TorA-PhoA translocation intermediate was, however, not affected by CCCP (*lane 16*) suggesting that its formation did not require the $\Delta\mu_H^+$. Interestingly, no translocation-arrested fragment of TorA-PhoA was obtained in the presence of DCCD (*lane 14*). This finding suggested that DCCD may also directly interfere with the Tat pathway prior to the two $\Delta\mu_H^+$-dependent steps (44).

To investigate this in more detail, the experiments shown in Fig. 5*C* were performed. As pointed out above, co-elution of oxidized TorA-PhoA with Tat$^+$-INV from Sepharose CL-6B reflects targeting to TatABC, which previously was found to be independent of $\Delta\mu_H^+$. Consequently, it was not perturbed by CCCP. Co-elution was, however, blocked by DCCD. The clear inhibition of membrane targeting by DCCD suggests that this compound must interfere with the interaction of TorA-PhoA with TatABC, possibly by covalently modifying essential carboxyl residues in TatC/TatB. Collectively, the results of Fig. 5 demonstrate that the translocation arrest of oxidized TorA-PhoA occurred subsequently to, and was dependent on, a func-

tional targeting to the TatABC translocase, but preceded a late $\Delta\mu_H{}^+$-sensitive translocation step.

Because the translocation arrest of TorA-PhoA was not perturbed by the uncoupler CCCP, it could actually be caused by a defective energization of the vesicles. We therefore re-isolated INV after allowing complete and partial translocation to occur (Fig. 5*D*, *lane 1*). These vesicles were subsequently incubated under conditions that allow formation of a $H^+$-gradient followed by digestion with PK (Fig. 5*D*, *lanes 2* and *3*). The vast majority of TorA-PhoA had accumulated as i-form and remained as such in the control sample, which did not receive any further additive (*lane 2*). Incubation in the presence of ATP, however, led to a significant increase in PK-protected, *i.e.* translocated precursor and mature form of TorA-PhoA at the expense of the i-form (*lane 3*). This indicates that part of the translocation-arrested TorA-PhoA could be fully translocated upon restoration of the $H^+$-gradient of the vesicles, and hence this material represents functional translocation intermediates.

*Translocation Arrest of Oxidized TorA-PhoA Occurs in the Immediate Proximity to TatA*—We next wished to find out if this translocation of oxidized TorA-PhoA, albeit being incomplete, nevertheless required the function of TatA. As shown in Fig. 6*A*, its accumulation was completely abolished not only in the absence of any Tat subunit (compare *lanes 2* and *8*), but also in membrane vesicles that selectively lack TatA (*lane 6*). The absence of the i-form from the PK-digest in *lanes 6* and *8* was not due to a decreased pool of precursor TorA-PhoA originating from an OmpT-dependent pseudo-processing seen with these vesicles (*lane 5* and *7*, *asterisk*). TatABC-containing INV obtained from such an *ompT*$^+$ *E. coli* strain, despite exhibiting substantial pseudo-processing (*lane 9*), nevertheless allowed detection of the translocation-arrested fragment (*lane 10*). Thus the translocation-arrested fragment of oxidized TorA-PhoA did not accumulate in the absence of TatA indicating that TorA-PhoA required TatA to enter the protease-protected environment.

Partial protection of oxidized TorA-PhoA was retained even after solubilization of INV by Triton X-100 (see Fig. 6*A*, *lane 4*). Resistance was also found toward other detergents such as $C_{12}E_9$, Chaps, and OG (Fig. 6*B*). This detergent resistance of the i-species of TorA-PhoA resembles the one described previously for TatA homo-oligomers (20, 45). We therefore investigated if translocation arrest in the membrane occurred close to TatA. To this end, oxidized TorA-PhoA was synthesized in the presence of Tat$^+$-INV to allow both complete translocation and generation of the translocation-arrested fragment (Fig. 6*C*, *lane 5*). The sample was subsequently digested with PK in the presence of 1% Triton X-100 to enrich for the translocation-arrested fragment (*lane 6*), which after inactivation of PK was applied to protein A-Sepharose-coupled antibodies directed against TatA, TatB, TatC, and PhoA (*lanes 7–10*). The translocation-arrested fragment of TorA-PhoA bound to the control anti-PhoA antibodies and to anti-TatA antibodies. Material released from both matrices displayed, however, a faster electrophoretic mobility than the i-species of TorA-PhoA. To demonstrate that this aberrant migration was caused by a high load of immunoglobulin molecules released from protein A-Sepharose, an identical experiment was performed (Fig. 6*D*), in which

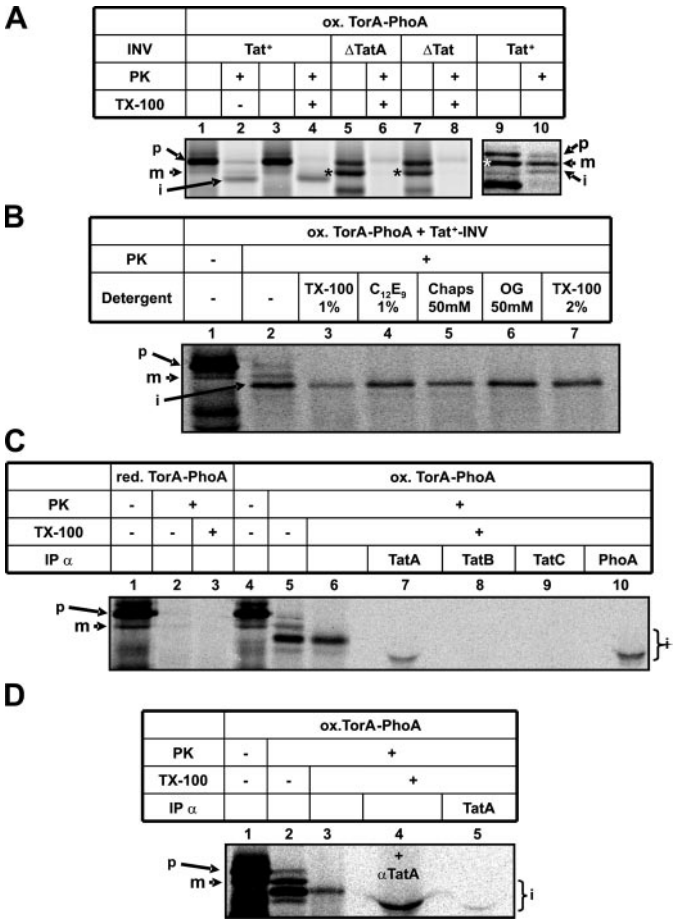


FIGURE 6. **Translocation arrest of TorA-PhoA occurs in the immediate proximity to TatA.** *A*, the translocation-arrested PK-fragment of TorA-PhoA accumulates neither in INV lacking TatABC (Δ*Tat*) nor in INV selectively devoid of TatA (Δ*TatA*). These INV being prepared from strain MC4100 (*ompT*$^+$) exhibit enhanced pseudo-processing of TorA-PhoA (*) compared with vesicles obtained from the *ompT*$^-$ BL21 strain (*lanes 1–4*). Pseudo-processing does, however, not interfere with the formation of the translocation-arrested fragment of TorA-PhoA as shown in *lanes 9* and *10*. *B*, the translocation-arrested PK-fragment of TorA-PhoA is resistant to a variety of detergents (*TX-100, $C_{12}E_9$, Chaps, OG*). *C*, the translocation-arrested fragment of oxidized TorA-PhoA was prepared by treatment with PK and Triton X-100 (*lane 6*) and following addition of 0.5 mM phenylmethylsulfonyl fluoride immunoprecipitated using antibody-loaded protein A-Sepharose. *D*, as *C*, except that in *lane 4*, the PK- and Triton X-100-resistant *i*-TorA-PhoA was mixed with anti-TatA antibodies prior to SDS-PAGE.

the enriched i-form of TorA-PhoA (*lane 3*) was mixed with anti-TatA serum prior to electrophoresis. As shown in *lane 4*, the mere addition of these antibodies led to the same displacement of the i-species on SDS-PAGE that it displayed after elution from protein A-Sepharose (compare *lane 4* to *lane 5* and to *lane 7* in *panel C*). We conclude from these findings that translocation-competent TorA-PhoA on its path across the cytoplasmic membrane of *E. coli* comes into close vicinity to TatA, where under the *in vitro* conditions employed here part of it becomes stalled.

## DISCUSSION

In this study, the fusion protein TorA-PhoA was used as a Tat-dependent precursor whose folding can deliberately be controlled by the redox state of the system. Folding of TorA-PhoA was induced by oxidized glutathione (GSSG), as Akiyama

and Ito (46) had shown that GSSG converts *in vitro* synthesized mature PhoA into an enzymatically active enzyme. Using a complete *in vitro* approach, we find that exclusively the oxidized form of TorA-PhoA is translocated into INV, a process that is entirely dependent on an active TatABC translocase of the vesicles. The latter is indicated by the findings that transport requires (i) high amounts of TatABC in the vesicles, (ii) an active RR motif in the TorA signal sequence, and (iii) the $\Delta\mu_H^+$ across the membrane; and that it is perturbed by the TorA-specific chaperone TorD. Although the TatABC translocase of the vesicles also allows binding of transport-incompetent, reduced TorA-PhoA, even if it carries an inactive KK motif, only the signal peptide of the oxidized RR counterpart could clearly be cross-linked to TatC and TatB. Binding to the Tat translocase does not require the $\Delta\mu_H^+$ but nonetheless is completely inhibited by DCCD. Even if translocation-proficient conditions were established in the *in vitro* system, *i.e.* employment of oxidized TorA-PhoA containing an intact RR motif and TatABC-containing INV, a substantial amount of TorA-PhoA was found arrested in a membrane-protected environment, leaving only the C terminus accessible to protease. Translocation arrest most likely results from an overload of the Tat translocase and has to be preceded by a productive interaction of TorA-PhoA with TatBC, but occurs prior to signal sequence cleavage and a $\Delta\mu_H^+$-dependent translocation step. Transmembrane stalling of TorA-PhoA requires the presence of TatA and takes place in immediate proximity to it. Translocation of a significant part of the arrested TorA-PhoA could be completed upon re-energization of the vesicles suggesting that at least part of it represents a functional transport intermediate.

As previously shown *in vivo*, the Tat translocase discriminates against unfolded TorA-PhoA (28). This concept was seemingly at odds with a report that unfolded RR-PhoA associated with TatABC (30), a finding that we have fully confirmed here. Different from the results of Richter and Brüser (30), we find unfolded TorA-PhoA even when harboring the inactive KK mutation to associate with TatABC in a manner that the precursor coelutes with INV from a gelfiltration column. Likewise, McDevitt *et al.* (20) also found overexpressed inactive RR variants of SufI associated with TatBC complexes expressed at wild-type levels and Alder and Theg (47) demonstrated cooperative binding of similar RR variants to the Tat translocase of plant thylakoids. In contrast, site-specific cross-linking of pre-SufI to *E. coli* TatC was completely, and that to TatB largely, abolished if the RR pair had been replaced by two consecutive lysine residues (13, 15). The same cross-linking method now revealed that the RR motif of transport-incompetent, reduced TorA-PhoA despite its binding to the Tat translocase, was not in genuine contact to TatC and TatB.

The obvious discrepancy between unrestricted targeting of transport-incompetent substrates to the Tat translocase and selection of active precursors by Tat(B)C could be explained if two subsequent binding steps to TatBC were postulated. A first, superficial targeting step would not exclusively depend on an intact RR pair, if it involved recognition of an extended sequence area within an RR signal peptide. Along this line, the recent isolation of distinct suppressor mutants in *tatB* and *tatC* that tolerate a KQ signal peptide and retain the ability to accept the RR wild type (17) suggests a large binding pocket with multiple contact points. Furthermore, less strictly conserved residues of the SRRxFLK consensus sequence likely contribute to the specificity of targeting (48, 49). Finally, contacts between the hydrophobic core of the SufI signal sequence and TatB were less strictly dependent on an intact RR motif than those between the consensus motif and TatBC (13).

Only in a second level of interaction would the RR consensus be directly juxtaposed to TatC as revealed by site specific cross-linking. We would predict that this recognition occurs deeper in the membrane. Recent findings indicate that an RR signal peptide must be able to interact with TatBC also within the plane of the lipid bilayer: some suppressor mutations of a KQ variant of TorA-MalE map to the N terminus of TatB predicted to lie on the *trans*-side of the membrane (17) as well as to a predicted periplasmic loop of TatC (18). Substitution of Phe for Val two residues downstream of the RR pair of the thylakoid precursor tOE17 results in a protease-resistant insertion of the signal sequence into the thylakoid Hcf106-cpTatC receptor (50), which together with other results prompted these authors to suggest a similar two-stage binding model.

Initial interaction of an RR precursor at surface-exposed sites of TatBC might cause conformational changes of TatBC that lead to an insertion of the signal sequence deep into the membrane and juxtaposition of the RR pair to Tat(B)C. In the case of TorA-PhoA, insertion requires both an intact RR motif and a folded conformation. Therefore, interlocked between those two discernable targeting steps sensing of the folding state must occur, most likely executed by TatBC. Richter *et al.* (2) have recently shown that Tat-dependent translocation is interrupted by surface-exposed hydrophobic patches and suggested that translocation might become halted when those hydrophobic side chains contact membrane lipids. According to our findings one could also speculate that recognition of hydrophobic patches as readout of a non-native protein structure might be recognized by TatBC.

A considerable amount of the *in vitro* synthesized TorA-PhoA stalled on its way across the membrane of the vesicles. Translocation arrest was indicated by a membrane-dependent, partial resistance to proteinase K. It strictly depended on a folded conformation of TorA-PhoA, the availability of an intact RR-motif, and prior recognition by the TatBC receptor complex. Importantly, it was not obtained in the absence of TatA, required the same spectrum of detergents for extraction from the membrane as TatA (20, 45), and accumulated in immediate proximity to membrane-embedded TatA. A similar translocation intermediate accumulating in a largely protease-protected thylakoidal membrane location was recently described for the RR fusion protein 23k-GFP whose signal sequence cleavage site had been mutated (51). Different from our findings, the 23k-GFP intermediate was not resistant to detergent extraction of the thylakoidal membrane and an interaction with Tha4, the TatA ortholog in plant chloroplasts, was not reported, which might reflect the more labile and transient nature of the thylakoidal Tha4 complex compared with bacterial TatA homooligomers (14, 22).

The reason for the translocation arrest of Tor-PhoA is not clear. Incomplete oxidation can be largely excluded, because all

TorA-PhoA precursor when synthesized in the presence of GSSG was resistant to alkylation and consequently oxidized. On the other hand, it is likely that the PhoA moiety of the TorA-PhoA fusion protein adopted a non-native conformation as indicated by the lack of any protease resistance in the absence of membranes, which clearly differs from mature, periplasmic PhoA. Impairment of folding of PhoA could be due to the presence of the TorA signal sequence and/or the seven amino acids from mature TorA upstream of authentic PhoA. Another possible explanation for translocation arrest of oxidized TorA-PhoA would be an overload of the TatABC translocase of the membrane vesicles, which has been demonstrated to occur both *in vitro* (39, 52) and *in vivo* (52). Irrespective of its cause, the fact that translocation arrest required prior intact targeting to TatBC and the strict availability of TatA, and that it could partially be released by re-installation of a $H^+$-gradient strongly suggest that it represents a step of the functional Tat pathway across the membrane bilayer. Except for previously shown contacts between the signal sequence of preSufI and TatA (13) our results are the first demonstration that TatA is recruited to a folded substrate that has functionally engaged the Tat translocase.

*Acknowledgments—We thank Dr. Peter Schultz, The Scripps Research Institute, La Jolla, for providing plasmid pDULE-pBpa, Drs. Tracy Palmer and Frank Sargent, University of Dundee, for plasmid pFAT222, pQE60-TorD, and antibodies against TorD, Dr. Jean-Michel Betton, Institut Pasteur, Paris, for antibodies against FkpA, and Adam Fisher for constructing plasmid pET28aTorA-PhoA.*

## REFERENCES


1. Hynds, P. J., Robinson, D., and Robinson, C. (1998) *J. Biol. Chem.* **273,** 34868–34874
2. Richter, S., Lindenstrauss, U., Lucke, C., Bayliss, R., and Brüser, T. (2007) *J. Biol. Chem.* **282,** 33257–33264
3. Cline, K., and McCaffery, M. (2007) *EMBO J.* **26,** 3039–3049
4. Blaudeck, N., Kreutzenbeck, P., Müller, M., Sprenger, G. A., and Freudl, R. (2005) *J. Biol. Chem.* **280,** 3426–3432
5. Barrett, C. M., Freudl, R., and Robinson, C. (2007) *J. Biol. Chem.* **282,** 36206–36213
6. McDevitt, C. A., Hicks, M. G., Palmer, T., and Berks, B. C. (2005) *Biochem. Biophys. Res. Commun.* **329,** 693–698
7. Oates, J., Barrett, C. M., Barnett, J. P., Byrne, K. G., Bolhuis, A., and Robinson, C. (2005) *J. Mol. Biol.* **346,** 295–305
8. Behrendt, J., Lindenstrauss, U., and Brüser, T. (2007) *FEBS Lett.* **581,** 4085–4090
9. Orriss, G. L., Tarry, M. J., Ize, B., Sargent, F., Lea, S. M., Palmer, T., and Berks, B. C. (2007) *FEBS Lett.* **581,** 4091–4097
10. Bolhuis, A., Mathers, J. E., Thomas, J. D., Barrett, C. M., and Robinson, C. (2001) *J. Biol. Chem.* **276,** 20213–20219
11. Lee, P. A., Orriss, G. L., Buchanan, G., Greene, N. P., Bond, P. J., Punginelli, C., Jack, R. L., Sansom, M. S., Berks, B. C., and Palmer, T. (2006) *J. Biol. Chem.* **281,** 34072–34085
12. Punginelli, C., Maldonado, B., Grahl, S., Jack, R., Alami, M., Schroder, J., Berks, B. C., and Palmer, T. (2007) *J Bacteriol* **189,** 5482–5494
13. Alami, M., Lüke, I., Deitermann, S., Eisner, G., Koch, H. G., Brunner, J., and Müller, M. (2003) *Mol Cell* **12,** 937–946
14. Cline, K., and Mori, H. (2001) *J. Cell Biol.* **154,** 719–729
15. Gerard, F., and Cline, K. (2006) *J. Biol. Chem.* **281,** 6130–6135
16. Holzapfel, E., Eisner, G., Alami, M., Barrett, C. M., Buchanan, G., Lüke, I., Betton, J. M., Robinson, C., Palmer, T., Moser, M., and Müller, M. (2007) *Biochemistry* **46,** 2892–2898
17. Kreutzenbeck, P., Kroger, C., Lausberg, F., Blaudeck, N., Sprenger, G. A., and Freudl, R. (2007) *J. Biol. Chem.* **282,** 7903–7911
18. Strauch, E. M., and Georgiou, G. (2007) *J. Mol. Biol.* **374,** 283–291
19. Barrett, C. M., Mangels, D., and Robinson, C. (2005) *J. Mol. Biol.* **347,** 453–463
20. McDevitt, C. A., Buchanan, G., Sargent, F., Palmer, T., and Berks, B. C. (2006) *FEBS J* **273,** 5656–5668
21. Greene, N. P., Porcelli, I., Buchanan, G., Hicks, M. G., Schermann, S. M., Palmer, T., and Berks, B. C. (2007) *J. Biol. Chem.* **282,** 23937–23945
22. Dabney-Smith, C., Mori, H., and Cline, K. (2006) *J. Biol. Chem.* **281,** 5476–5483
23. Gohlke, U., Pullan, L., McDevitt, C. A., Porcelli, I., de Leeuw, E., Palmer, T., Saibil, H. R., and Berks, B. C. (2005) *Proc. Natl. Acad. Sci. U. S. A.* **102,** 10482–10486
24. Gouffi, K., Gerard, F., Santini, C. L., and Wu, L. F. (2004) *J. Biol. Chem.* **279,** 11608–11615
25. Chan, C. S., Zlomislic, M. R., Tieleman, D. P., and Turner, R. J. (2007) *Biochemistry* **46,** 7396–7404
26. Mori, H., and Cline, K. (2002) *J. Cell Biol.* **157,** 205–210
27. Brüser, T., and Sanders, C. (2003) *Microbiol. Res.* **158,** 7–17
28. DeLisa, M. P., Tullman, D., and Georgiou, G. (2003) *Proc. Natl. Acad. Sci. U. S. A.* **100,** 6115–6120
29. Sanders, C., Wethkamp, N., and Lill, H. (2001) *Mol. Microbiol.* **41,** 241–246
30. Richter, S., and Brüser, T. (2005) *J. Biol. Chem.* **280,** 42723–42730
31. Matos, C. F., Robinson, C., and Di Cola, A. (2008) *EMBO J.* **27,** 2055–2063
32. Fisher, A. C., Kim, W., and DeLisa, M. P. (2006) *Protein Sci.* **15,** 449–458
33. Hatzixanthis, K., Clarke, T. A., Oubrie, A., Richardson, D. J., Turner, R. J., and Sargent, F. (2005) *Proc. Natl. Acad. Sci. U. S. A.* **102,** 8460–8465
34. Farrell, I. S., Toroney, R., Hazen, J. L., Mehl, R. A., and Chin, J. W. (2005) *Nat. Methods* **2,** 377–384
35. Moser, M., Panahandeh, S., Holzapfel, E., and Müller, M. (2007) *Methods Mol. Biol.* **390,** 63–80
36. Studier, F. W., Rosenberg, A. H., Dunn, J. J., and Dubendorff, J. W. (1990) *Methods Enzymol.* **185,** 60–89
37. Casadaban, M. J., and Cohen, S. N. (1979) *Proc. Natl. Acad. Sci. U. S. A.* **76,** 4530–4533
38. Wexler, M., Sargent, F., Jack, R. L., Stanley, N. R., Bogsch, E. G., Robinson, C., Berks, B. C., and Palmer, T. (2000) *J. Biol. Chem.* **275,** 16717–16722
39. Alami, M., Trescher, D., Wu, L. F., and Müller, M. (2002) *J. Biol. Chem.* **277,** 20499–20503
40. Sargent, F., Stanley, N. R., Berks, B. C., and Palmer, T. (1999) *J. Biol. Chem.* **274,** 36073–36082
41. Hoffmann, J. H., Linke, K., Graf, P. C., Lilie, H., and Jakob, U. (2004) *EMBO J.* **23,** 160–168
42. Jack, R. L., Buchanan, G., Dubini, A., Hatzixanthis, K., Palmer, T., and Sargent, F. (2004) *EMBO J.* **23,** 3962–3972
43. Chin, J. W., Martin, A. B., King, D. S., Wang, L., and Schultz, P. G. (2002) *Proc. Natl. Acad. Sci. U. S. A.* **99,** 11020–11024
44. Bageshwar, U. K., and Musser, S. M. (2007) *J. Cell Biol.* **179,** 87–99
45. de Leeuw, E., Granjon, T., Porcelli, I., Alami, M., Carr, S. B., Müller, M., Sargent, F., Palmer, T., and Berks, B. C. (2002) *J. Mol. Biol.* **322,** 1135–1146
46. Akiyama, Y., and Ito, K. (1993) *J. Biol. Chem.* **268,** 8146–8150
47. Alder, N. N., and Theg, S. M. (2003) *FEBS Lett.* **540,** 96–100
48. Stanley, N. R., Palmer, T., and Berks, B. C. (2000) *J. Biol. Chem.* **275,** 11591–11596
49. Mendel, S., McCarthy, A., Barnett, J. P., Eijlander, R. T., Nenninger, A., Kuipers, O. P., and Robinson, C. (2008) *J. Mol. Biol.* **375,** 661–672
50. Gerard, F., and Cline, K. (2007) *J. Biol. Chem.* **282,** 5263–5272
51. Di Cola, A., and Robinson, C. (2005) *J. Cell Biol.* **171,** 281–289
52. Yahr, T. L., and Wickner, W. T. (2001) *EMBO J.* **20,** 2472–2479